16th World Conference on Earthquake Engineering, 16WCEE 2017
Santiago Chile, January 9th to 13th 2017
Paper N° 2752 (Abstract ID)
Registration Code: S-V1460788377

Cyclic Loading Test of Reinforced Concrete Frame with Partial Wall having Steel Damper

Y. Maida [1], H. Sakata [2], N. Izumi [3], T. Maegawa [4], M. Hamada [5]

[1] *Assistant Professor, Dept. of Architecture, Chiba University, yusuke.maida@chiba-u.jp*
[2] *Professor, Dept. of Architecture and Building Engineering, Tokyo Institute of Technology, sakata.h.aa@m.titech.ac.jp*
[3] *Professor, Dept. of Architecture, Chiba University, nobuyuki.izumi@faculty.chiba-u.jp*
[4] *Manager, Technical Research & Development Institute, Kumagai Gumi Co., Ltd., tmaegawa@ku.kumagaigumi.co.jp*
[5] *Deputy General Manager, Technical Research & Development Institute, Kumagai Gumi Co., Ltd., mhamada@ku.kumagaigumi.co.jp*

Abstract

The structural performance of the non-structural wall in reinforced concrete (RC) frames has attracted much attention in Japan. There are several types of non-structural walls such as spandrel wall, partition wall, wing wall, and partial wall. In the past, a non-structural wall has been connected rigidly to the column and beam without providing the structural slit. However, this causes adverse effects to the RC frame, such as shear failure of the short column with spandrel and partition walls. In recent years, providing a structural slit has become common. As a result, the non-structural wall causes no adverse effects to the RC frame when a structural slit is employed. In addition, the structural slit is mostly used to simplify a design. On the other hand, a non-structural wall with a structural slit is not expected to provide strength.

This study focuses on the partial wall in RC frames. The application of a steel slit damper in a partial wall is proposed, as it makes a non-structural wall contribute to seismic performance and utilizes the structural slit effectively. The steel slit dampers applied are hysteretic dampers, which dissipate energy by the flexural yielding of the edge of the steel. Some of the benefits from these dampers include the possibility of energy dissipation resulting from a small displacement, its malleability, and its low-cost manufacturing potential.

In this paper, the seismic performance of the RC frames with a partial wall having a steel damper is investigated through cyclic loading tests. Four specimens were used in this study. The first specimen is a partial wall in an RC frame, which is connected to the RC beam without a structural slit (RW). The second specimen is a partial wall in an RC frame with a structural slit (SW). Its partial wall is separated from the RC beam by the structural slit. The third specimen is a steel damper installed in the lower part of the partial wall in RC frames (LD). The fourth specimen is a steel damper installed in the central part of the partial wall in RC frames (CD). The connection between the steel damper and the RC beam is fixed by embedding the PC bar into the RC beam. The connection between the steel damper and the partial wall is fixed by head studs.

The specimens with the partial wall having steel dampers LD and CD yield and start to dissipate energy at an early stage, with story drift ratios much smaller than those at beam yielding. However, the difference in the damper horizontal deformation has occurred between the positive and negative loading at the large deformation zone. Based on the damage of the RC frame and the partial wall, the LD and CD specimens have a greater damage control effect than the RW specimen.

Keywords: non-structural RC wall, structural slit, steel damper, energy dissipation, equivalent viscous damping factor

1. Introduction

From the earthquake damage survey in recent years, damage of non-structural walls in reinforced concrete (RC) has been reported [1]. For non-structural walls, there is a damage control method to separate the beam-to-column frames by the structural slit. However, structures were designed expecting the excessive ductility of a ramen frame, and as plastic deformation occurs at the time of a large earthquake, the continued use of the residual deformation is difficult. On the other hand, wing walls, spandrel walls, etc., that have been treated as non-structural walls previously, have been treated in recent years as structural resistance elements by rigid connection beam-to-column frames, increasing the strength of the building [2]. Non-structural walls that have a rigid connection to the RC frame suffer a brittle fracture after demonstrating strength in the small deformation zone (Fig. 1 (a)). From the viewpoint of increasing the strength of the entire building and ensuring energy dissipation capabilities, currently it is not necessarily advantageous to place a structural slit.

This study focuses on partial walls as non-structural walls and proposes a damage control structure according to the damper application to the partial walls. By placing a damper on the structure slit position of the partial wall, the damper is yielded at an earlier stage than the beam-to-column frame in order to suppress the damage to the partial wall and beam-to-column frames and to improve the energy dissipation capacity of the entire building (Fig. 1 (b)). Shiohara et al. [3] shows the effectiveness of the energy dissipation capacity granted by the dowel rebar joining the precast wall and beam-to-column frames.

In this study, the structural behavior of the RC frames of applying the energy dissipation device in the partial walls make clear and its design method establish. As a first step, a subassemblage test of the RC frame with a partial wall with an applied damper is carried out. From the test results, quantitative evaluation of the energy dissipation capability and equivalent viscous damping factor is performed. In addition, damage control effects of the beam-to-column frames and partial wall is confirmed.

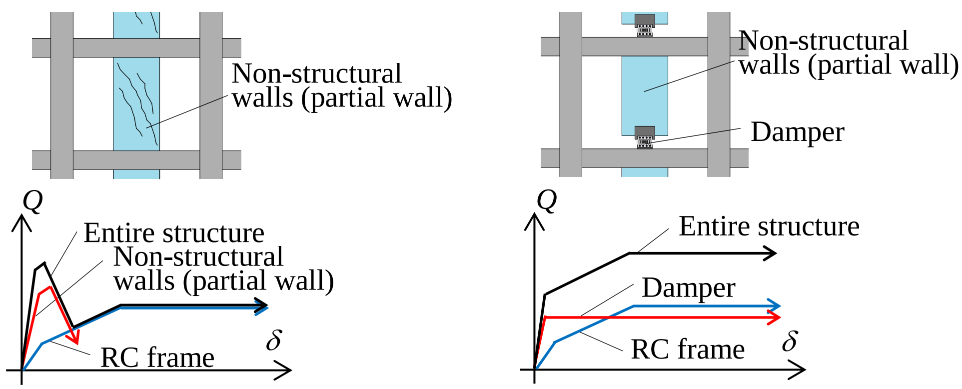

(a) Non-structural walls that are rigid connection to the RC frame

(b) Application of damper to the non-structural walls in RC frame

Fig. 1 – Properties of the frames due to the difference in the treatment of non-structural walls

2. Experimental Program

2.1 Outline of specimen

The details of the specimens are shown in Fig. 2. The specimen parameters, properties, and material properties of concrete are listed in Table 1. The material properties of rebar and steel are listed in Table 2. The specimens were 1/2 scale of the RC beam, and a column subassemblage frame with a partial wall that resembles the trial design of a middle-rise RC building.

The RC part was detailed in accordance with the latest standard of the Architectural Institute of Japan for concrete structures [4]. The column had a square cross-section of 300 × 300 mm. It was reinforced by 18-ϕ13 longitudinal rebars, resulting in a 2.5% gross reinforcement ratio; and ϕ6 double hoops at 50 mm spacing, resulting in 0.85% transverse reinforcement ratio. The beam cross-section was 350 mm in height and 175 mm in width. It was symmetrically reinforced by 6-ϕ13 longitudinal rebars, with a 1.5% reinforcement ratio for bending; and ϕ6 one and a half stirrups at 75 mm spacing, resulting in 0.72% transverse reinforcement ratio. The axial force in the column was not introduced.

The cross-section of the partial wall and the reinforcement of the specimen that does not install the dampers was the same as the common ones. If the strength of this partial wall was calculated by using the "Commentary of Japanese Building Code for Structural Safety" [5], when the axial force acting on the partial wall is assumed to be zero, it is calculated as a bending fracture. On the other hand, in the actual building, elongation of the partial wall is restrained around the frames. As a result, the axial force ratio of 0.15 is equivalent to the compression axial force that is applied to the partial wall [6]. If it is considered, it is calculated as a shear fracture.

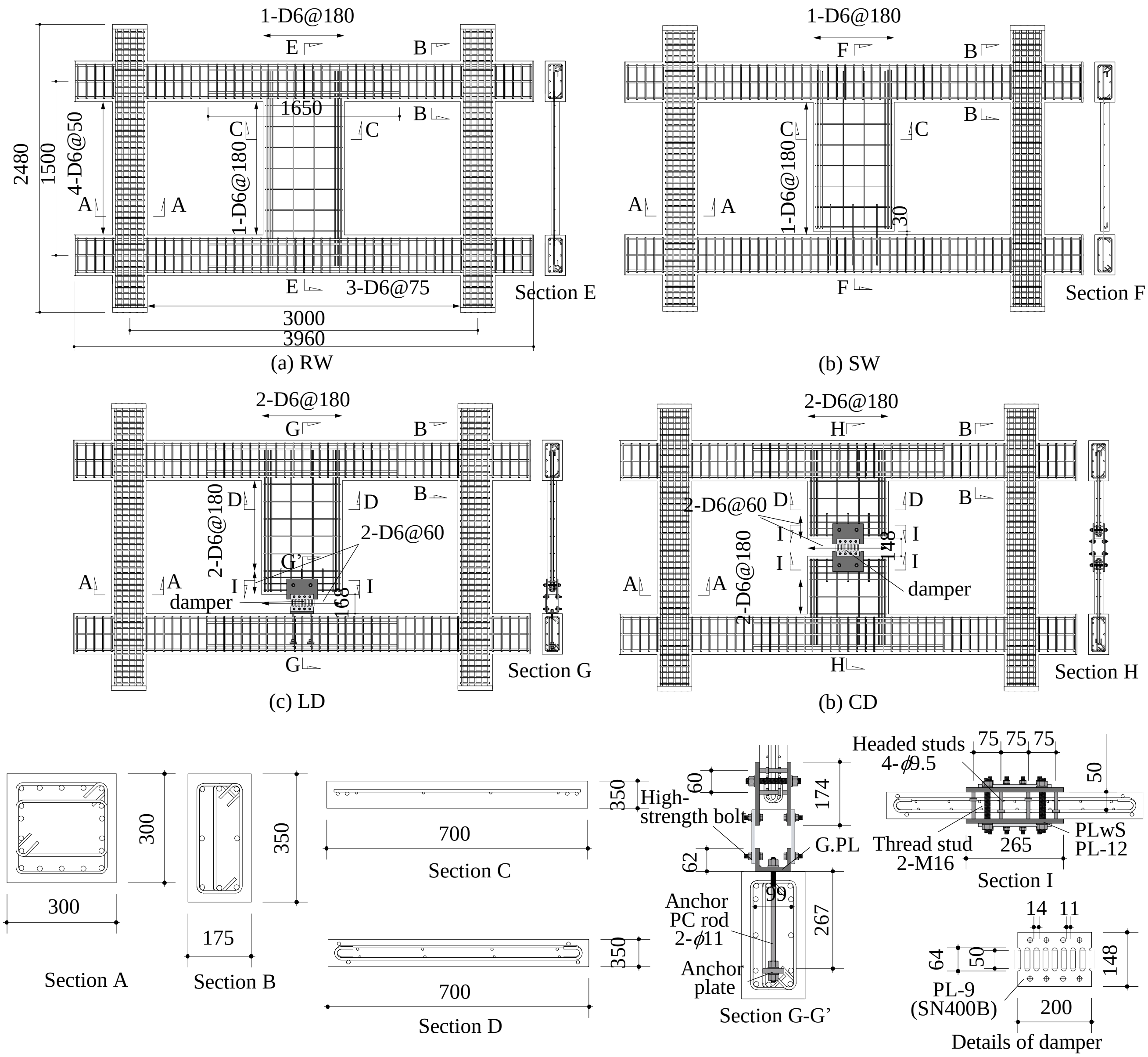

Fig. 2 – Details of specimens

Table 1 – Specimen parameters, properties, and material properties of concrete

			RW	SW	LD	CD
Column	Dimensions (mm)		300×300			
	Longitudinal rebar		18-D13 (SD345) p_g=2.54%			
	Hoop		4-D6@50 (SD295A) p_w=0.85%			
Beam	Dimensions (mm)		175×350			
	Longitudinal rebar	Edge	3-D13 (SD345) p_t=0.73%			
		Central	3+2-D13 (SD345)	3-D13 (SD345)	3+2-D13 (SD345)	
	Stirrups		3-D6@75 (SD295A) p_w=0.72%			
Partial wall	Dimensions (mm)		75×700			
	Stirrups		1-D6@180 (SD295A) p_w=0.23%		2-D6@180 (SD295A) p_w=0.47%	
	Opening reinforcement		2-D10 (SD295A)			
	Stirrups around damper connection		-		2-D6@60 (SD295A) p_w=1.41%	
All members	$\sigma_B/\sigma_T/E_C$ (N/mm²)		52.9/3.78/34000	54.3/4.21/34200	56.0/4.35/34400	48.4/3.82/32900

σ_B: Concrete compressive strength, σ_T: Concrete tensile strength, E_C: Concrete elastic modulus

Table 2 – Material properties of rebar and steel

	Yield strength (N/mm²)	Tensile strength (N/mm²)	Young's modulus (N/mm²)
Longitudinal rebar D13 (SD345)	381	535	190000
Opening reinforcement D10 (SD295A)	371	513	194000
Hoop, Stirrups D6 (SD295A)	430	553	184000
Steel of damper PL-9 (SN400B)	290	426	185000

The partial wall of the specimen that installed the dampers were designed using the above equations [5] so as not to shear failure relative to the damping force. In addition, the connection around the damper increased the amount of reinforcement.

The damper used was a steel slit damper [7]. The yield strength of the damper is designed as 50 kN. This is about 2/3 of the yield strength calculated value of RC beam-column frames. The story drift ratio during damper yielded was designed approximately as 1/800 rad for when there is no deformation loss in the damper connection.

The major difference among the specimens was the presence or absence of a structural slit in the partial walls, as well as the presence or absence of the damper in partial walls. Four specimens were tested. First, the partial wall with a rigid connection to the beam (RW); second, the partial wall was separated from RC frames by placing the structural slit at the lower end (SW); third, the damper was installed to the structural slit of the partial wall at the lower end (LD); and fourth, the damper was installed to the structural slit of the partial wall at the center (CD).

The dampers are mounted in pairs, so that the partial wall is interposed. On the partial wall, two steel plates, which have welded headed studs (PLwS), are attached and interposed from the front and the back. In addition, they were fixed by a continuous thread stud 2-M16 for the purpose of preventing vertical and horizontal displacement (section I). The headed stud has been designed based on the “Design Recommendations for Composite Structures” [8] for the damper yield strength. It used a stud of steel plate on one side per 4-ϕ9.5.

On the beam, a gusset plate (G.PL) was post-tensioned and connected by the anchor PC rod. The prestressing bolts for fastening the gusset plate were designed to be prestressed to a total of 140 kN, which has determined the friction coefficient between RC beams and G.PL as 0.4 [9] by the yield strength of the two dampers (50 kN) so as not to cause displacement in G.PL. In other words, each anchor bolt in the group was prestressed to 70 kN.

2.2 Loading

The test setup is shown in Fig. 3. The top and bottom of the column were supported by pins. The pin bearing at the bottom of the column attached to the reaction force floor. The pin bearing at the top of the column is connected to the actuator through the loading jig. There was positive and negative cyclic loading. Cyclic loading with increasing displacement amplitudes was conducted. For each specimen, two cycles were carried out for story drift ratio amplitudes of 1/1600, 1/800, 1/400, 1/200, 1/100, 1/67, and 1/50 rad. After that, only one cycle was carried out for the amplitude of 1/33 rad. Finally, only one positive cycle was carried out for the amplitude of 1/25 rad.

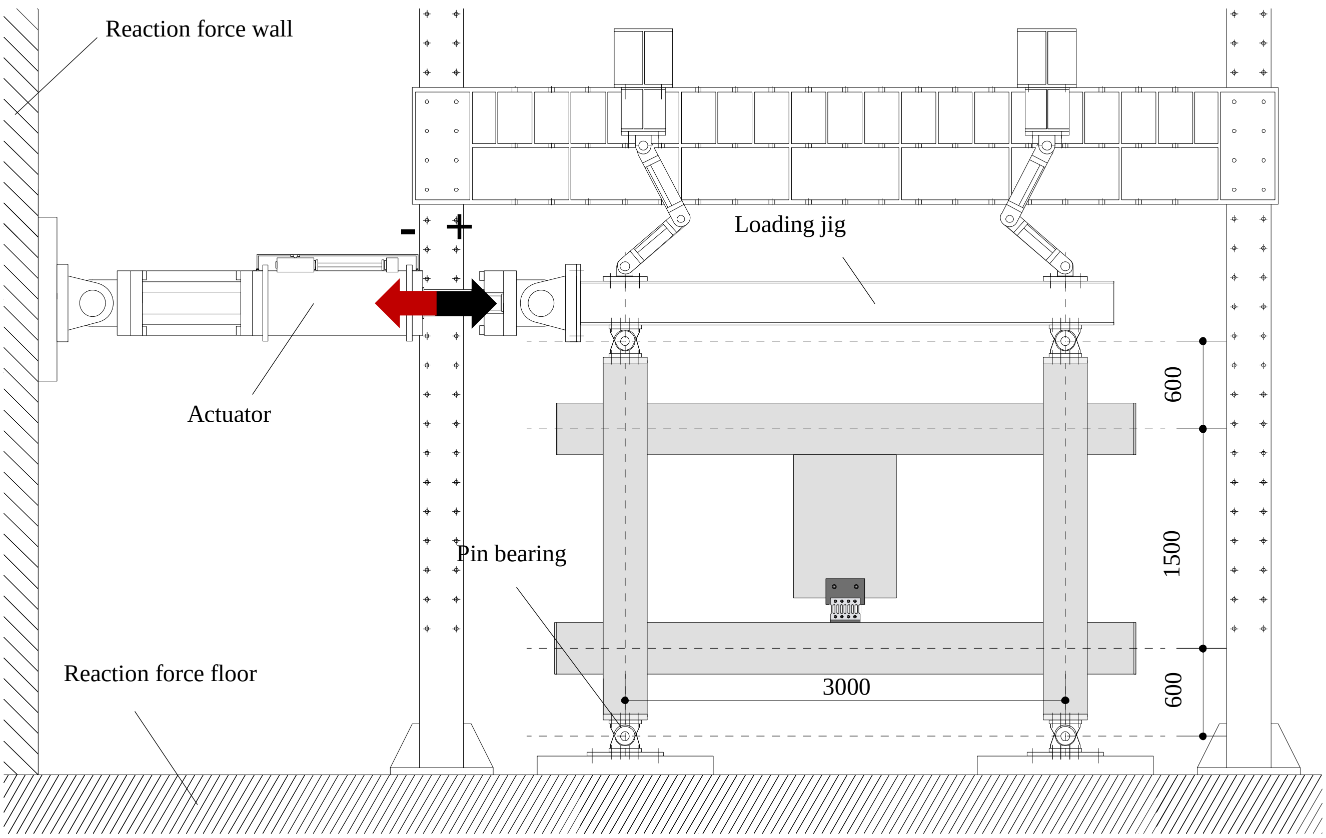

Fig. 3 – Test setup

3. Experimental Results

3.1 Story drift ratio-story shear force relation

The story drift ratio *R* versus story shear force *Q* relationship is shown in Fig. 4.

For RW, the maximum story shear force reached 160 kN in 1/255 rad, and the partial wall was shear failure. The hysteresis loop of RW was obtained similarly to SW in the subsequent loading. For SW, the yield of the beam rebar is confirmed in 1/219 rad, and the maximum story shear force reached 125 kN in 1/25 rad. It had a stable hysteresis characteristic until the end of the test. The sway rebar of the partial wall was broken during the 1/67 rad cycle.

For LD, and CD, the damper yielded in each test at 1/673 and 1/1080 rad, and the beam rebar yielded in each test at 1/223 and 1/240 rad. The maximum story shear force was confirmed respectively as 171 and 167 kN. The final fracture type of RC frames in both specimen was confirmed as bending fracture of the beam.

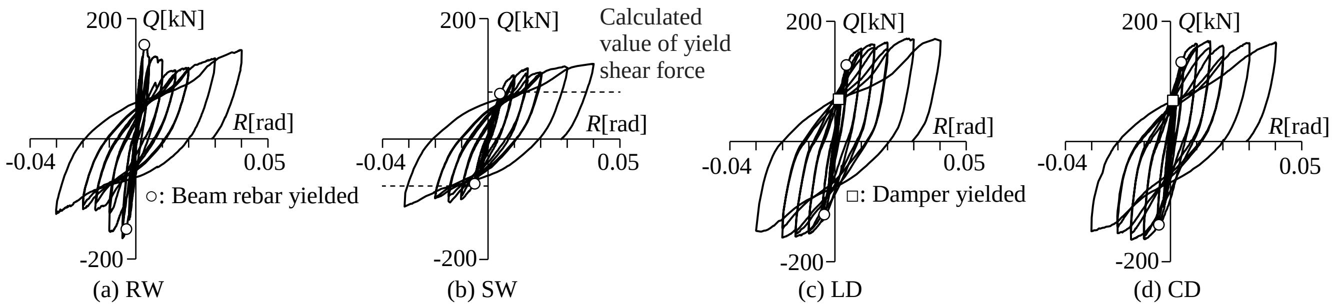

Fig. 4 – Story drift ratio versus story shear force

3.2 Energy dissipation capability and equivalent viscous damping factor

The accumulative hysteretic energy dissipation *E* is shown in Fig. 5.

At *R* = -1/100 rad, the energy dissipated was as follows: *E* = 6.7 kNm in RW, *E* = 3.5 kNm in SW, *E* = 7.9 kNm in LD, and *E* = 9.9 kNm in CD. In addition, at the end of the test, the energy dissipated was as follows: *E* = 36.0 kNm in RW, *E* = 31.1 kNm in SW, *E* = 50.5 kNm in LD, and *E* = 49.7 kNm in CD. There was very little difference in the energy dissipation amount at the end of the test for LD and CD. They were obtained approximately 1.4 times SW and 1.6 times RW.

From the information above, by applying the damper into the partial wall which designed in consideration of the damping force can be ensured a stable energy dissipation capacity.

Next, the equivalent viscous damping factor is observed. The equivalent viscous damping factor in each cycle of 1/800, 1/400, 1/200, 1/100 rad are listed in Table 3.

In the 1/400 rad cycle, the equivalent viscous damping factor of the CD specimen is remarkable. The damper yields at an early stage and, it is granted the high damping effect from a small deformation zone. In the 1/200 rad cycle, the equivalent viscous damping factor was confirmed as about 2 times in RW, LD, CD specimens as compared to the SW specimen. In the 1/100 rad cycle, both LD and CD specimens showed the same equivalent viscous damping factor, approximately 13%.

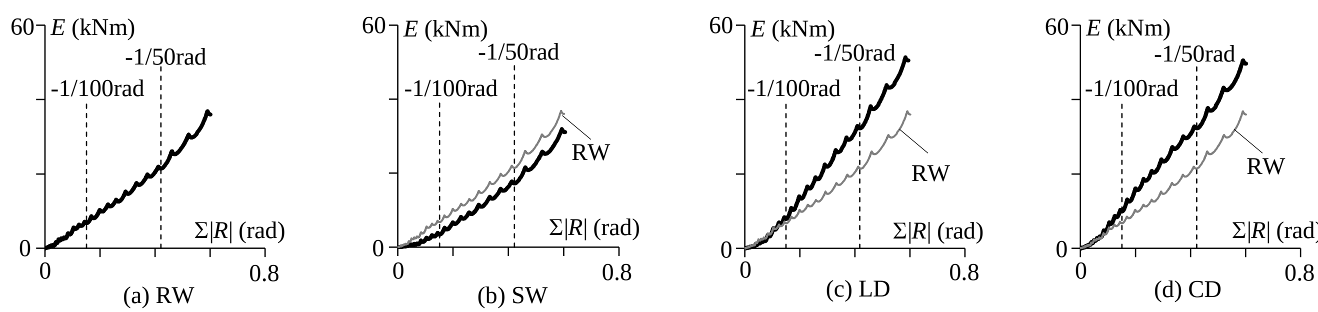

Fig. 5 – Accumulative hysteretic energy dissipation

Table 3 – Equivalent viscous damping factor in each cycle of 1/800, 1/400, 1/200, 1/100 rad

Cycle (rad)	RW	SW	LD	CD
1/800	6.1	6.0	6.7	6.7
1/400	5.1	5.8	5.5	8.3
1/200	8.1	4.3	7.8	9.6
1/100	10.9	10.4	12.7	13.1

3.3 Crack patterns and transition of crack width

The crack patterns at the story drift ratio *R* = -1/100 rad unloading point of all specimens are shown in Fig. 6.

The specimens, with the exception of RW, had flexural cracks on the beam ends at an early stage. Afterwards, flexural-shear cracks accompanied the increase of the story drift ratio. Next, the partial wall is observed. Flexural cracks were confirmed at the time of *R* = 1/67 rad in SW. For LD and CD, flexural cracks occurred at the time of *R* = 1/800 rad, and shear cracks occurred *R* = 1/400 rad. On the other hand, for RW, flexural cracks and shear cracks were confirmed at the time of *R* = 1/1600 rad. With increasing story drift ratio, the shear crack width of the partial walls increased. The partial wall showed shear fractures in the *R* = 1/200 rad cycle.

Maximum crack width of the beam and the partial wall at the peak point and unloading point of each loading cycle are shown in Fig. 7.Fig. 7 shows the classification of the limit state and the degree of damage that are shown in the “Guidelines for Performance Evaluation of Earthquake Resistant Reinforced Concrete Buildings (Draft)” [10]. It shows a 1/2 of the actual index in consideration of dimensional effect of the specimen. The crack width was measured with the crack scale (minimum scale 0.05 mm). The maximum crack width of the beam, at the time of *R* = 1/200 rad unloading, is beyond the limits available in RW. For LD and CD, the crack width was within use limit. During *R* = 1/100 rad unloading, it exceeds the repair limit in LD and CD. By attaching the damper, residual deformation is increased owing to the difference in unloading stiffness for the RC frame and damper.

Then, the maximum crack width of the wall is observed. For RW, it is beyond the “use limit” at the time of *R* = 1/400 rad unloading, and it has been evaluated as “repair limit II” at the time of *R* = 1/200 rad unloading. For LD and CD, the crack width is kept smaller than for the RW in the all story drift ratios.

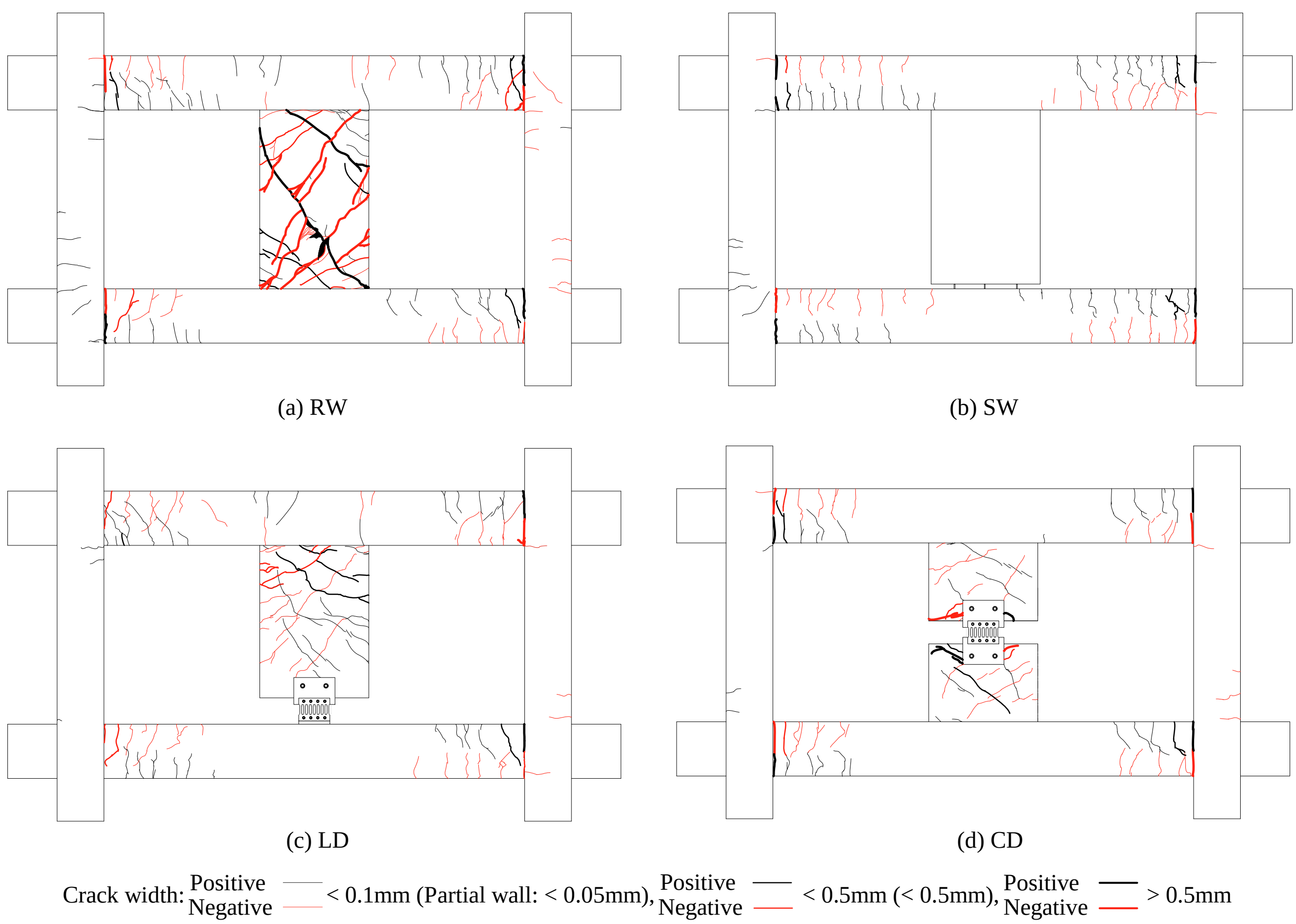

Fig. 6 – Crack patterns at story drift ratio *R* = -1/100 rad unloading point

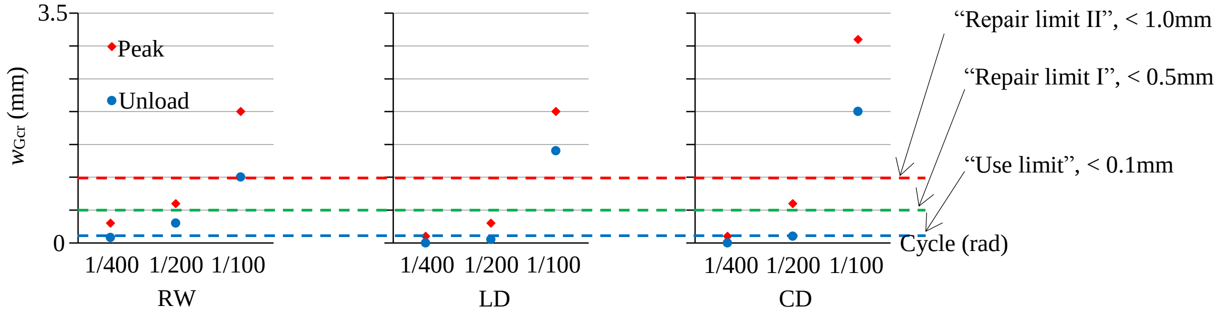

(a) Maximum crack width of the beam

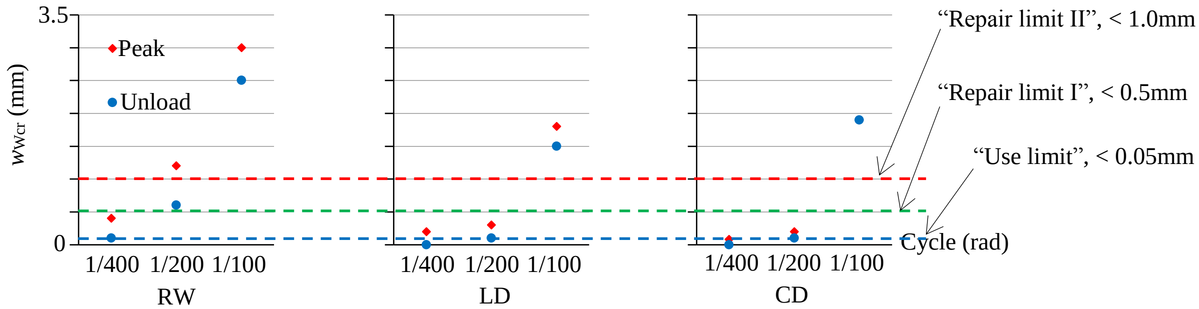

(b) Maximum crack width of the partial wall

Fig. 7 – Transition of crack width

3.4 Behavior of damper and damper connection

In this section, the behavior of the damper and damper connection for LD and CD are discussed. The displacement measurement positions are shown in Fig. 8 (i).

By focusing on the state of the story shear force at the time of R = 1/100 rad cycle, the story shear force is positive loading (■-◆), positive unloading (◆−□), negative loading (□-◇), and negative unloading (◇-Δ).These are considered the behavior in each state. The horizontal axis in Fig. 8 is a cumulative story drift ratio. For all the figures, results are shown up to R = 1/67 rad unloading point.

3.4.1 Behavior of damper

The horizontal deformation of the damper is shown in Fig. 8 (ii).

The horizontal deformation of the damper is not much different in the positive and negative loading in the small deformation zone. However, the difference of horizontal deformation of the damper has occurred between the positive and negative loadings at the large deformation zone. It is considered to be affected by deformation of the damper connection and the cracks on the partial wall.

3.4.2 Displacement of PLwS

The horizontal displacement of PLwS is shown in Fig. 8 (a) (iii), (b) (iii), and (b) (iv). The vertical displacement of PLwS is shown in Fig. 8 (a) (iv).

The horizontal displacement of PLwS is increased or decreased with the increase or decrease of the story shear force. For LD, the horizontal displacement of PLwS occurs below a maximum of 0.4 mm, and the displacement is almost reduced to zero at the unloading point. For CD, the horizontal displacement of PLwS occurs up to a maximum of 5.0 mm, and the displacement is gradually biased to the negative side. The vertical displacement of PLwS increased or decreased significantly during positive side loading and unloading, and it occurs during negative side loading and unloading. The horizontal displacement of the damper is not stabilized by the deformation loss of the damper connection because of the damage of the concrete around the headed. In order to ensure a stable damper displacement, there is a need for further consideration about the details of the damper connection to partial walls.

3.4.3 Displacement of G.PL

The horizontal displacement of G.PL is shown in Fig. 8 (a) (v). The vertical displacement of G.PL is shown in Fig. 8 (a) (vi).

The horizontal displacement of G.PL occurred below the maximum of 0.2 mm. It can be ignored because it is small relative to the horizontal deformation of the damper. On the other hand, the vertical displacement of G.PL occurred during positive and negative loading, with the residual displacement occurring even if unloading. Therefore, in G.PL, it is necessary to ensure a higher initial introduction tension of the prestressing bolts.

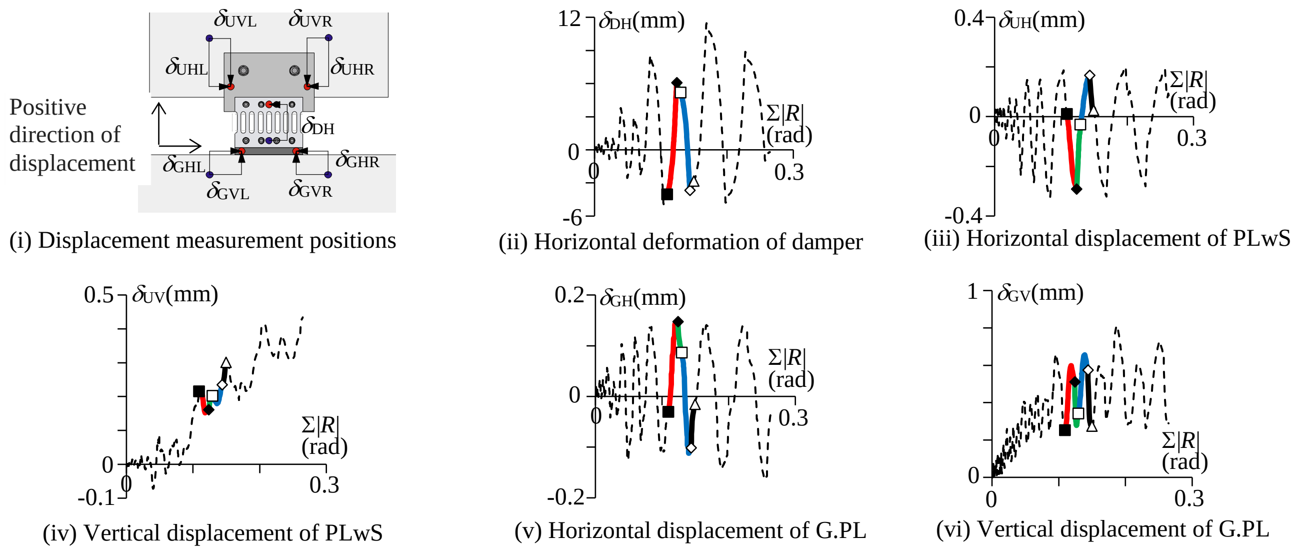

(i) Displacement measurement positions
(ii) Horizontal deformation of damper
(iii) Horizontal displacement of PLwS
(iv) Vertical displacement of PLwS
(v) Horizontal displacement of G.PL
(vi) Vertical displacement of G.PL

(a) LD

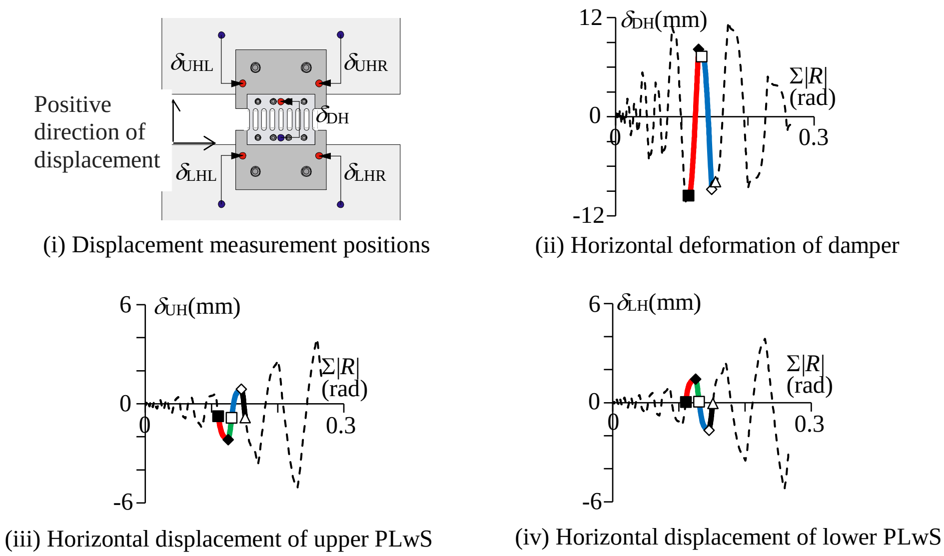

(i) Displacement measurement positions
(ii) Horizontal deformation of damper
(iii) Horizontal displacement of upper PLwS
(iv) Horizontal displacement of lower PLwS

(b) CD

Fig. 8 – Behavior of damper and damper connection

4. Conclusions

In this study, cyclic loading tests on RC frames with a partial wall having a steel damper were conducted. It is confirmed by the test results that the specimens of partial wall having a steel damper ("LD" and "CD") yield and start to dissipate energy at an early stage with story drift ratios much smaller than those at beam yielding. However, the difference of horizontal deformation of the damper has occurred between the positive and negative loading at the large deformation zone. It is considered to be affected by the deformation of the damper connection and the cracks on the partial wall. Focusing on the damage of the RC frame and the partial wall, the LD and CD specimens have a greater damage control effect than the RW specimen. Therefore, by applying the damper into the partial wall, a stable energy dissipation capacity and damping effect can be ensured.

5. Acknowledgements

This work was supported by the Program to Disseminate Tenure Tracking System, MEXT, Japan, and the Grants-in-Aid for Research Activity Start-up (15H06094), JSPS KAKENHI. The representative is Yusuke Maida. These financial supports are gratefully acknowledged.

6. References

[1] Architectural Institute of Japan (2011): Preliminary Reconnaissance Report of the 2011 Tohoku-Chiho Taiheiyo-Oki Earthquake [in Japanese]

[2] Fukuyama H., Kabeyasawa T., Mukai T., Suwada H., Tajiri S., Tani M., Teshigawara M., Kusunoki K. (2015): Static Loading Test on A Full Scale Five Story Reinforced Concrete Building utilizing Wing Walls for Damage Reduction, Part 1. Outline of the Full Scale Test, Summaries of technical papers of AIJ annual meeting, Architectural Institute of Japan, **C-2**, 361-362. [in Japanese]

[3] Shiohara H. (2006): Development of Non-structural Jointed Precast Concrete Panel for Earthquake response control, Summaries of technical papers of AIJ annual meeting, Architectural Institute of Japan, **C-2**, 121-124. [in Japanese]

[4] Architectural Institute of Japan (2010): AIJ Standard for Structural Calculation of Reinforced Concrete Structures [in Japanese]

[5] Building Guidance Division, Housing Bureau, Ministry of Land, Infrastructure, Transport and Tourism et al. (editor) (2007): Commentary of Japanese Building Code for Structural Safety [in Japanese]

[6] Tani, M., Mukai, T., Ogura, M., Taleb, R., and Kono, S. (2014): Full-scale Experiment on Non-structural R/C Walls Focused on Failure Modes and Damage Mitigation, Second European Conference on Earthquake Engineering and Seismology, ID 656, 1-12.

[7] Nakamura H., Ono Y., Sugiyama S., Wada A., Baba M., Miyabara T. (1997): Passive control system using steel slit damper, Part 1. Test of Steel slit damper, Summaries of technical papers of AIJ annual meeting, Architectural Institute of Japan, **B-2**, 843-844. [in Japanese]

[8] Architectural Institute of Japan (2010): Design Recommendations for Composite Structures [in Japanese]

[9] Architectural Institute of Japan (2011): Stress Transferring Mechanism and Resistance Mechanism of Steel-Reinforced Concrete Joints [in Japanese]

[10] Architectural Institute of Japan (2004): Guidelines for Performance Evaluation of Earthquake Resistant Reinforced Concrete Buildings (Draft) [in Japanese]